# Sensorless adaptive optics for microscopy

Alexander Jesacher[a] and Martin J. Booth[b]

[a] Division of Biomedical Physics, Innsbruck Medical University, Austria
[b] Department of Engineering Science, University of Oxford, U.K.

## 1. INTRODUCTION

The imaging properties of a microscope suffer from the presence of aberrations and optimum performance is obtained only when aberrations are zero. As aberrations are introduced by imperfections in the optical system or by the inhomogeneous refractive index distribution of the specimen, most microscope systems are in some way affected. In order to ensure optimum image quality, optical systems are designed so that the overall aberration is set below an acceptable tolerance. However, if the system is used outside of its design specifications, including when the specimen refractive index differs from the objective immersion medium, then aberrations can be significant. Correction of these aberrations through adaptive optics is essential if optimum imaging performance is to be ensured.

In adaptive optics (AO), an adaptive element, such as a deformable mirror, is used to introduce additional wavefront distortions that cancel out other aberrations in the system. Traditional adaptive optics systems, such as those developed for astronomical telescopes, also use a wavefront sensor to measure aberrations. Common methods for direct wavefront sensing are the Shack-Hartmann sensor[1] or devices based on interferometry.[2] An advantage of these sensors is their speed, which makes them methods of choice for astronomical or free-space optical communication applications, where corrections have to be performed at the fast timescale given by air turbulence.

Whilst adaptive optics techniques have been applied to microscopy, most of these systems have not used wavefront sensors, but have instead relied upon indirect aberration measurements[3] (Fig. 1). One reason for this is that, for many microscopy applications, it is not straightforward to apply direct wavefront sensing due to the three-dimensional nature of the specimen. The sensor would ideally detect light emanating from the focal region, but light is instead emitted from a larger three-dimensional region of the specimen. As most wavefront sensors have no mechanism for discriminating between in-focus and out-of-focus light, the sensor readings can be ambiguous. For this reason, most adaptive microscope systems have been "sensorless" AO systems, in which the correction aberration is inferred from a collection of image measurements, where each image is acquired with a different aberration introduced by the adaptive element. We refer to these additional aberrations as "bias aberrations". As in any AO system, the goal of a sensorless AO system is to find a DM shape that cancels all other aberrations in the system, or at least reduces them to an acceptable level. The sensorless AO scheme must therefore be able to determine from a set of aberrated images what the optimal correction aberration is or, equivalently, what the system aberration is. We explore the principle behind this approach. We also describe the methods that can be used to design efficient sensorless adaptive schemes by appropriate choice of aberration modes.

## 2. INDIRECT WAVEFRONT SENSING

As aberrations affect the imaging quality of a microscope, some information about the nature of the aberrations must be encoded in the images. One should expect therefore that some of this information could be extracted indirectly from an aberrated image or, more readily, from a collection of aberrated images. This is the principle behind sensorless AO.

This review article has been published in similar form as a chapter in the book "Adaptive Optics for Biological Imaging", J. Kubby (ed.), CRC Press, 2013.

E-mail: martin.booth@eng.ox.ac.uk

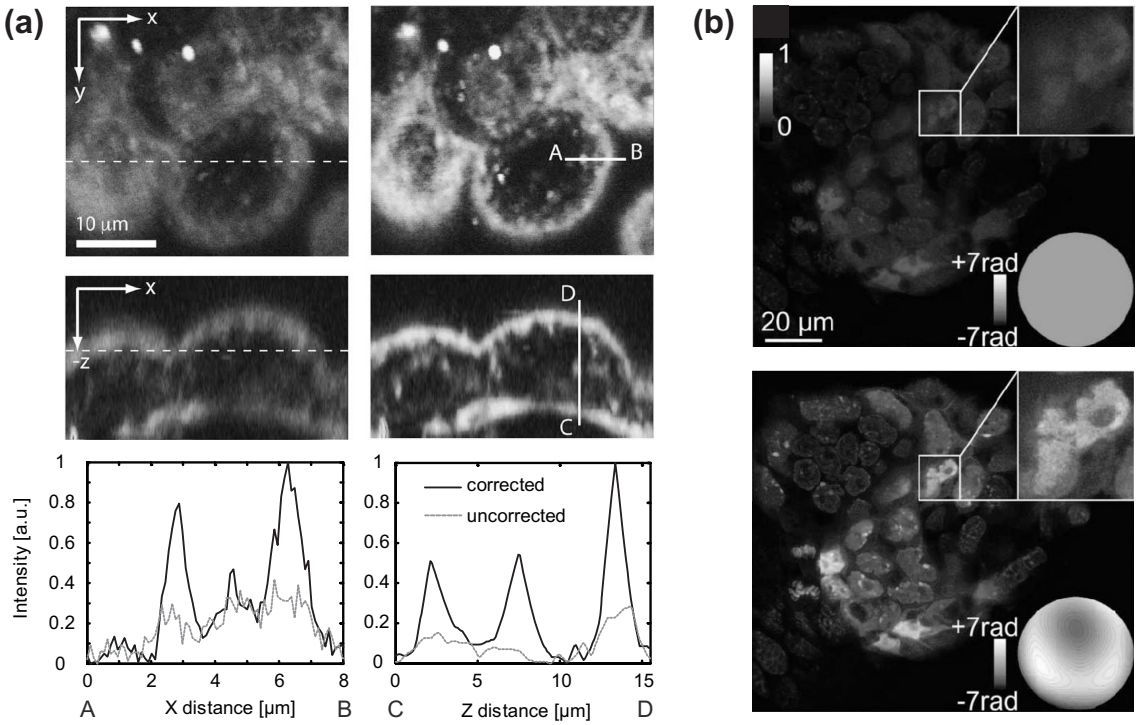


Figure 1. Examples of the correction of aberrations in multiphoton microscopes using sensorless adaptive optics. (a) Third harmonic generation images of a 5.5 day old live mouse embryo with correction of only system aberrations (left) and after additional correction of specimen-induced aberrations (right). The dashed lines show where the xy and xz planes intersect. Also shown are intensity profiles along the solid lines AB and CD as drawn in the images. (Reproduced from Jesacher *et al.*[4]) (b) Two-photon excitation fluorescence images of a mouse embryo: upper, before correction; lower, after correction) . (Reproduced from Débarre *et al.*[5])

Mathematically speaking, an image is a function of both the object structure and the imaging properties of the microscope. For example, in the case of a confocal fluorescence microscope (an incoherent imaging system), the image is the convolution of the fluorophore distribution in the object and the intensity point spread function (PSF) of the microscope. As the aberrations affect only the imaging properties, the sensorless AO scheme must be able to separate this information from the effects of the object structure. Phase retrieval methods have been used to extract aberration information from a single image, but these methods are effective only if the object structure is known (for example, if the specimen is a single point-like bead).[6] For unknown specimen structures, the aberrations can only be determined by acquiring more images, each with a different bias aberration introduced by the adaptive element. Assuming that the object structure is unknown but does not change between image measurements, then comparisons between the quality of the biased images should reveal the effects of the aberrations on the imaging properties of the microscope. This information about image quality forms the basis for determination of the aberration in the system and consequently the optimum setting for the correction element.

The definition of "image quality" is somewhat subjective. However, there are many ways in which quality can be reasonably represented by a mathematical quantity. For example, in the confocal fluorescence microscope, the magnitude of the intensity PSF is reduced as the size of aberration increases; consequently, the total image intensity (the sum of all pixel values) is also reduced. It is straightforward to show that for most object structures the total image intensity is maximum when aberrations are zero. Hence the total image intensity is an appropriate metric for representation of image quality in this microscope.

Once we have defined an appropriate image quality metric, we can consider the sensorless AO scheme as a mathematical optimization problem, whose objective is to maximize the metric function, which we denote as $M$. The maximum of $M$ corresponds to the optimum DM setting that minimizes the total aberration in the system. The metric $M$ is a function of input parameters that determine the aberration applied by the adaptive element.

These input parameters can be represented by the set of $P$ control signals $\{c_1, \ldots, c_P\}$ driving the actuators of the DM. The calculation of the image quality for each applied aberration is therefore equivalent to evaluation of the metric function at the coordinates given by the DM control signals. The objective of the optimization is therefore to find the values of $c_1, \ldots, c_P$ that maximize $M(\{c_1, \ldots, c_P\})$.

The general outline of this optimization procedure is shown in Fig. 2. There exist many different strategies for the implementation of this procedure, including the various heuristics used in convex optimization theory. One possible approach is to use model-free stochastic methods, for which we need to assume only that $M$ has a well defined maximum value. For example, one could test all possible shapes of the DM and select the setting with optimum image quality – this would be equivalent to an exhaustive search through all possible aberrations represented by all possible combinations of control signals. Whilst from a mathematical point of view this is guaranteed to find the optimum correction, the number of image measurements would be impractically large.[7] Other more developed model-free methods, such as genetic or hill climbing algorithms, have been demonstrated.[8,9] Whilst they are more efficient than an exhaustive search, they typically require a large number of image measurements. Whilst in principle the acquisition of these images in possible, there are several reasons why this is incompatible with practical microscopy. Specimens are often sensitive to cumulative light exposure – live specimens suffer from photo-toxic effects and even fixed fluorescent specimens undergo photo-bleaching. Many multiple exposures are clearly undesirable in each of these cases. Specimens may also move during the imaging sequence, hence the specimen structure will not stay constant. It is therefore desirable to minimize the measurement time by ensuring that the number of exposures is as small as possible.

Using the mathematical analogy, each specimen exposure (and quality metric calculation) corresponds to a function evaluation in the optimization problem. It follows that reducing the required number of exposures is equivalent to the derivation of an efficient optimization algorithm that minimizes the number of function evaluations. This can be achieved using *a priori* knowledge of how aberrations influence the metric through, for example, a functional description the microscope's image formation process in the presence of aberrations.

In the following sections, we show how the appropriate mathematical formulation of the optimization problem informs the design of the sensorless AO scheme. In particular, we show how the choice of the modal expansion used to represent aberrations plays an important role in the efficiency of the process.

## 3. MODAL REPRESENTATION OF ABERRATIONS

In the previous section, we explained how the optimization metric $M$ can be represented as a function of the control signals that drive the actuators of the deformable mirror. However, it is usually more convenient to express a wavefront as a sequence of basis functions or aberration modes. For example, an arbitrary wavefront $\Phi(r,\theta)$ is expressed as

$$\Phi(r,\theta) = \sum_i a_i X_i(r,\theta), \tag{1}$$

with $a_i$ representing the mode coefficients and $X_i$ the basis functions. If the deformable mirror is used in a linear operating regime, then the modal coefficients are related to the DM control signals by a linear transformation.

The aim of modal wavefront sensing is to obtain the coefficients $a_i$ directly. This contrasts with zonal sensing methods, like the Shack-Hartmann sensor, where the measured wavefront is constructed from separate measurements from different regions of the wavefront.[1] The choice of the basis modes $X_i$ can be influenced by various factors, both mathematical and practical. For example, Zernike polynomials are often used for systems with circular apertures as they form a complete, orthogonal set of functions defined over a unit circle.[10,11] The expansion may also be based upon the deformation modes of a deformable mirror or the statistics of the induced aberrations. For an efficient sensorless AO scheme, the modal expansion is chosen to ensure that the metric function has certain mathematical properties. These are discussed in the next section.

## 4. SENSORLESS ADAPTIVE OPTICS USING MODAL WAVEFRONT SENSING

In the design of an efficient sensorless AO scheme, we should use *a priori* knowledge of the form of the optimization metric $M$ as a function of the mode coefficients $a_i$. In most practical situations, this form is approximately

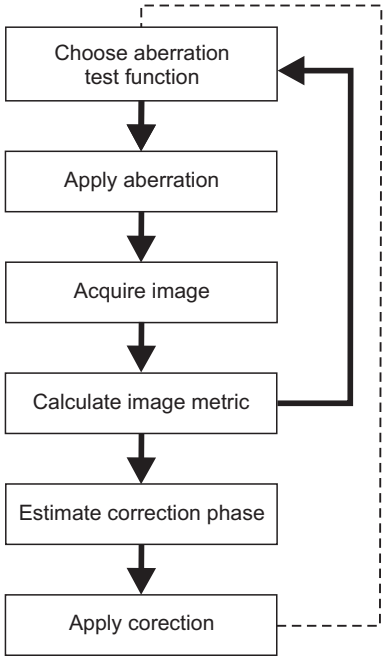


Figure 2. Flow chart of the indirect wavefront sensing scheme. A sequence of images is acquired, each with a different aberration applied. For each image, the quality metric is calculated. From the obtained metric values the correction phase is estimated. The dashed line represents an optional repeat of the process, if full correction was not achieved after the first cycle.

parabolic in the vicinity of the maximum of $M$. This observation assists us in designing an efficient optimization algorithm that uses minimal function evaluations and hence fewest specimen exposures. We will first show the principle of this approach in a system where only one aberration mode is present. In the subsequent discussion we extend this description to the case of multiple aberration modes.

## 5. MEASUREMENT OF A SINGLE MODE

When only one aberration mode $X_i$ is present in the system, then the aberrated wavefront can be expressed as $\Phi(r,\theta) = aX_i(r,\theta)$ and the optimization problem is equivalent to a one-dimensional maximization of a parabolic function. Close to its maximum, the metric $M$ can be expressed as

$$M \approx M_0 - \alpha\ a^2 \tag{2}$$

where $a$ denotes the aberration mode coefficient and $\alpha$ is constant. The metric has the maximum value $M_0$ when the aberration coefficient $a$ is zero. The values of $M_0$ and $\alpha$ are usually unknown, as they depend upon factors such as specimen structure, illumination intensity and detection efficiency. Let us now include the effect of an adaptive element that adds the aberration $cX_i(r,\theta)$. Equation 2 then becomes

$$M \approx M_0 - \alpha\ (a+c)^2 \tag{3}$$

where it is clear that $M$ is maximum when $c = -a$ and the correction aberration fully compensates the system aberration. As we are free to choose the value of $c$, the right hand side of Eq. 2 contains three unknown variables, one of which, $a$, we wish to determine. It follows that we can extract the value of $a$ from three measurements of $M$ that we obtain using different values of $c$. To achieve this practically, bias aberrations corresponding to three different values of $c$ are intentionally introduced to the wavefront and the corresponding metric values are measured. This process proceeds as follows. The first step requires taking an image with zero additional aberration applied by the adaptive element ($c = 0$). The metric value $M_Z$ is calculated from the resulting image. Subsequently, two further measurements are taken, with small amounts $c = \pm b$ of the bias aberration introduced

to the system. The corresponding images provide the metric values $M_+$ and $M_-$. We then use a simple quadratic maximization algorithm to find the aberration magnitude $a$ from the three metric measurements:[12]

$$a = -\frac{b(M_+ - M_-)}{2M_+ - 4M_Z + 2M_-} \tag{4}$$

From this, the necessary correction amplitude is obtained as $c = -a$. This measurement principle is illustrated in Fig. 3.

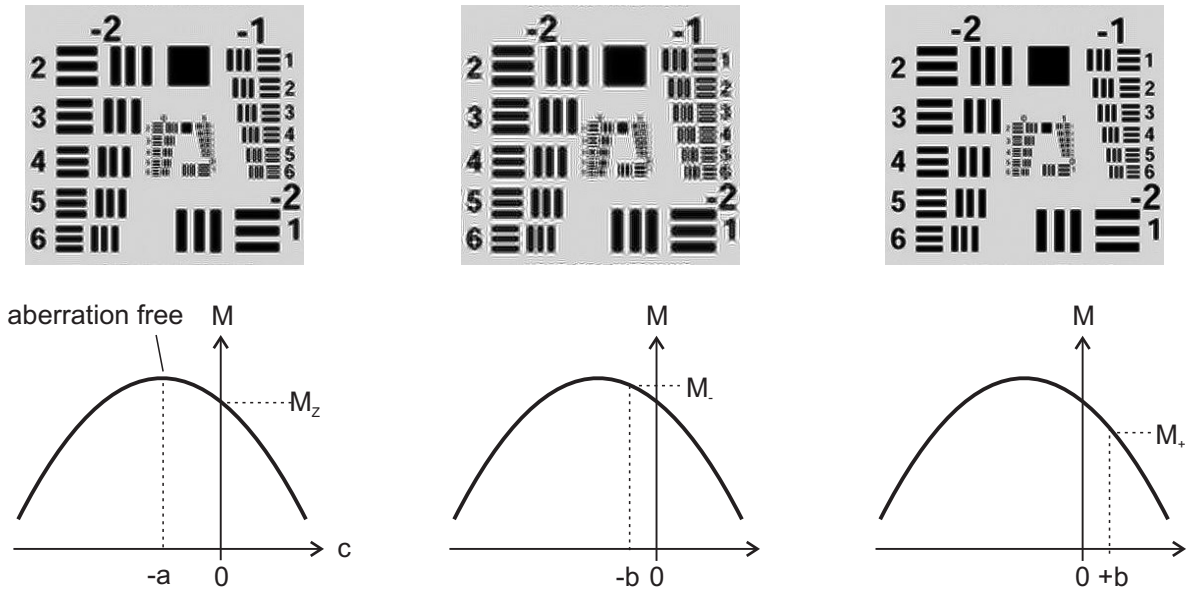


Figure 3. Principle of modal wavefront sensing of a single aberration mode. Three images are acquired with intentionally applied bias aberrations $-b$, 0 and $+b$ and the corresponding metric values $M_-$, $M_Z$ and $M_-$ are calculated from the images. The aberration magnitude $a$ is then derived from the three metric values using a quadratic maximization calculation.

## 6. MEASUREMENT OF MULTIPLE MODES

When multiple aberration modes are present in the system, then $\Phi(r,\theta) = \sum_i a_i X_i(r,\theta)$ and the optimization problem is equivalent to a multi-dimensional maximization of a paraboloidal function. Using a Taylor expansion around the maximum point, where $a_i = 0$ for all $i$, the metric $M$ can be expressed in a general form as

$$M \approx M_0 - \sum_i \sum_j \alpha_{i,j}\ a_i\ a_j \tag{5}$$

where $M_0$ and $\alpha_{i,j}$ are unknown constants. The one dimensional quadratic maximization approach of the previous section is not obviously extendable to this more complicated multidimensional function. In particular, we see that the coefficients for each mode do not appear as separable terms in the Taylor expansion. If we consider the shape of the metric function, this means that the primary axes of the paraboloid do not align with the coordinate axes formed by the coefficients $a_i$. This is illustrated in Fig. 4a using the simple case where two aberration modes are present. Performing an optimization in one aberration coefficient will find the maximum along a section parallel to the coordinate axes. Repetition of this process for the second aberration coefficient leads to a combined correction aberration for both modes. However, this does not find the overall maximum of the paraboloid (although further repetition of the process would move the correction closer to the optimum value).

In practical terms this effect means that a standard set of basis modes, such as the Zernike polynomials, will not in general be the best choice for control of a sensorless adaptive microscope. Indeed, it has been found

that each different type of microscope would have its own ideal set of modes, which do permit independent optimization of each mode using the quadratic optimization method.

The non-ideal basis modes can be converted by recasting Eq. 5 through a coordinate transformation so that the coordinate system is aligned with the paraboloid. The metric can then be expressed as

$$M \approx M_0 - \sum_i \beta_i \; d_i^2 \tag{6}$$

where the variables $d_i$ are new coordinates derived from the original coordinates $a_i$ and the constants $\beta_i$ are related to the constants $\alpha_{i,j}$ of Eq. 5. This coordinate transformation is equivalent to the derivation of a new set of aberration modes $Y_i(r,\theta)$, each of which is a linear combination of the original modes $X_i(r,\theta)$. The total aberration can therefore be expressed in terms of either set of modes as $\Phi(r,\theta) = \sum_i a_i X_i(r,\theta) = \sum_i d_i Y_i(r,\theta)$. Methods for derivation of the new modes are discussed in Section 8.

As each aberration coefficient $d_i$ appears in a separate term on the right hand side of Eq. 6, it is possible to employ the one-dimensional quadratic maximization in sequence to each separate coefficient. As these calculations are mutually independent, only one maximization per mode is necessary to find the peak of the metric function. This is illustrated for the two mode system in Fig. 4b. The orientation of the coordinate axes with the axes of the paraboloid ensures that the correction aberration is found efficiently with the smallest number of maximization cycles. We can therefore consider the choice of modes $Y_i$ as being optimum for this system.

The single mode maximization procedure presented in the last section required three measurements with bias aberrations corresponding to $c = -b,\ 0,\ b$. This procedure can be applied in turn to each of the multiple aberration modes. It appears therefore that maximization of $M$ when $N$ aberration modes are present would require $3N$ measurements. However, as the bias aberration corresponding to $c = 0$ is common to all modes, the total number of measurements can be reduced to $2N + 1$. This is illustrated in Fig. 4c.

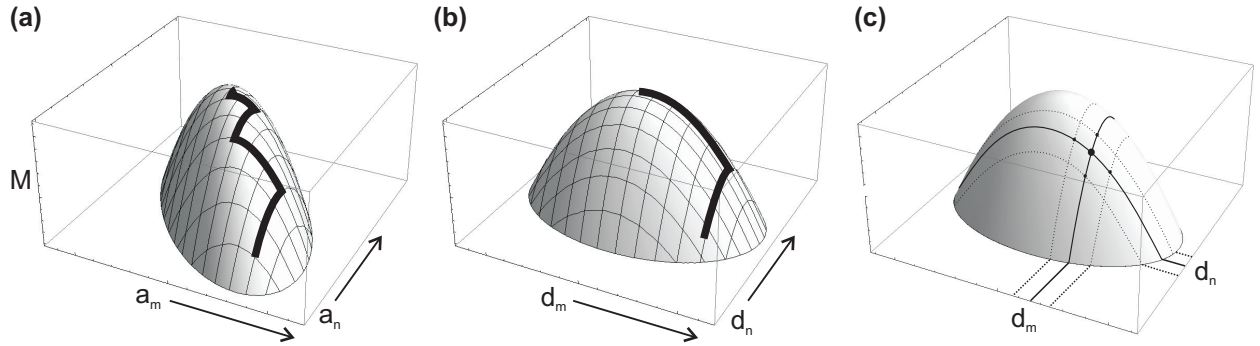


Figure 4. (a) Principle of modal wavefront sensing for a system with two basis modes $X_m$ and $X_n$. Maximization with respect to these modes is not optimal and several cycles are required to reach the peak. (b) The equivalent process for the derived modes $Y_m$ and $Y_n$. As the axes of the paraboloid are aligned with the coordinate axes, the maximization of each mode is independent and the peak is obtained after a single measurement cycle. (c) Schematic illustration of the biased aberration measurements for the two mode system. The positions of the five dots represent the aberration biases required for the measurements. This set of measurements is sufficient to reconstruct the whole paraboloid and hence to determine the correction aberration.

## 7. EXAMPLE OF A SENSORLESS ADAPTIVE SYSTEM

In this section we illustrate the principles of sensorless modal wavefront measurement using a simple adaptive optical system, as shown in Fig. 5. The measurement system consists of an adaptive element, a convex lens, a sub-wavelength-sized pinhole and a photo-detector. The intensity of the light passing through the pinhole is chosen as the optimization metric. This is an appropriate choice as the measured intensity will be maximal for an aberration-free beam. We derive analytic expressions showing how the metric depends upon the aberrations in the system and we demonstrate how choosing specific properties of the aberration modes allow its simplification to the form given in Eq. 6.

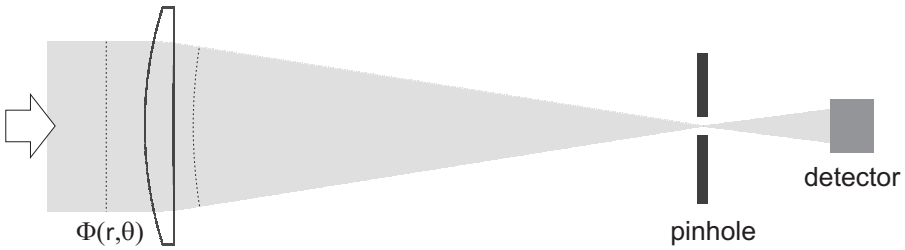


Figure 5. Simple sensorless adaptive system consisting of an aberrated input beam, a focusing lens and a pinhole detector.

The intensity at the pinhole plane is given by the modulus squared of the Fourier transform of the pupil field:

$$I(\nu,\xi) = \left| \frac{1}{\pi} \int\int P(r,\theta) \exp\left[\iota r \nu \cos(\theta - \xi)\right] r \; dr \; d\theta \right|^2 \tag{7}$$

where $\iota$ is the imaginary unit, $(\nu, \xi)$ are the polar coordinates in the pinhole plane and $P(r,\theta)$ is the pupil function. It is assumed that the pupil is circular with unit radius, so that $P(r,\theta) = 0$ for $r > 1$. Assuming that the intensity of the input beam is uniform, we define $P(r,\theta) = \exp\left[\iota \Phi(r,\theta)\right]$. In the limit of a point-like pinhole, the metric (the signal measured by the photodetector) is proportional to the on-axis intensity, which is found by setting $\nu = 0$ in Eq. 7. The metric takes a relatively simple form:

$$M = \left| \frac{1}{\pi} \int_r^1 \int_\theta^{2\pi} \exp\left[\iota \Phi(r,\theta)\right] r \; dr \; d\theta \right|^2 \tag{8}$$

If the aberration amplitude is small, the exponent can be expanded to give

$$M = \left| \frac{1}{\pi} \int_r^1 \int_\theta^{2\pi} \left[ 1 + \iota \Phi(r,\theta) - \frac{1}{2}\Phi(r,\theta)^2 + ... \right] r \; dr \; d\theta \right|^2 \tag{9}$$

Using the aberration expansion of Eq. 1 in the above equation yields

$$M = \left| 1 + \frac{\iota}{\pi} \sum_i a_i \int\int X_i \; r \; dr \; d\theta - \frac{1}{2\pi} \sum_i \sum_j a_i a_j \int\int X_i X_j \; r \; dr \; d\theta + ... \right|^2 \tag{10}$$

where for notational brevity we have omitted the explicit dependence of $X_i$ on $(r,\theta)$. The second term on the right hand side of the equation can be set to zero if we assume that the aberration modes $X_i$ have zero mean value. This assumption is reasonable in practice as it is equivalent to choosing modes do not contain any piston component. As piston has no effect on the metric measurement, this assumption does not restrict us in any practical way. The metric can then be written as

$$M \approx 1 - \sum_i \sum_j \alpha_{i,j} a_i a_j \tag{11}$$

where we define

$$\alpha_{i,j} = \frac{1}{\pi} \int\int X_i X_j \; r \; dr \; d\theta \tag{12}$$

Equation 11 is now in the same form as Eq. 5. The integral on the right hand side of Eq. 12 has the properties of an inner product between modes $X_i$ and $X_j$. Indeed, this inner product is identical to that defining the orthogonality of the Zernike polynomials. We can also note that the value of $\alpha_{i,j}$ in Eq. 12 can equivalently be obtained by calculating the partial derivative of the metric:

$$\alpha_{i,j} = \frac{\partial M}{\partial a_i \partial a_j} = \frac{1}{\pi} \int\int X_i X_j \; r \; dr \; d\theta \tag{13}$$

If the modes $X_i$ are chosen appropriately, then one can ensure that the modes are orthonormal and $\alpha_{i,j} = \delta_{i,j}$ with $\delta_{i,j}$ being the Kronecker delta. Equation 11 simplifies to

$$M \approx 1 - \sum_i a_i^2 \tag{14}$$

which has the desired form of Eq. 6, where each coefficient can be maximized independently of the others.

We have seen that for this sensorless adaptive system, an efficient scheme can be derived if the modes are orthogonal according to the definition of the inner product in Eq. 12. The Zernike polynomials form a set of modes that fulfil this property. However, one is free to use other sets of modes that have similar mathematical properties but are better suited to a specific application. This approach is outlined in the next section.

## 8. DERIVATION OF OPTIMAL MODES

The example system described in Section 7 illustrates how the required modal properties can be extracted from a mathematical expression for the optimization metric. In principle, this approach can be applied to more complex sensorless adaptive systems, such as adaptive microscopes using image-based quality metrics. However, the increased complexity of the mathematics describing the imaging process means that simple expressions for the inner product are not readily obtained. Similarly, conventional analytic modal sets, such as the Zernike polynomials, may not have the required mathematical properties. Generally, it is necessary to derive new sets of modes for a particular application to ensure optimal performance of the sensorless system. Three different methods that have been used to obtain optimum modes in these systems – analytical, numerical and empirical – are explained below.

1. *Analytical:* In some situations, it is possible to define a set of analytic functions that are orthogonal with respect to the inner product. This method has been employed, for example, using Zernike modes in a focussing system[7] (as described in Section 7) or Lukosz modes in a focussing system[13] or in an incoherent microscope using image low spatial frequency content as the metric.[14] This analytical approach is of relatively limited application, as there are few sets of known analytic modes that could be matched to any particular adaptive system.

2. *Numerical:* If the functional form of the inner product is known, for example from the Taylor expansion or by direct evaluation of $\frac{\partial M}{\partial a_i \partial a_j}$, then the optimum orthogonal modes can be obtained numerically. As a starting point, one selects a suitable set of modes as a basis set (e.g. a subset of low-order Zernike polynomials). The optimum modes are then constructed from the basis set using an orthogonalization process based around the inner product. This has been shown in structured illumination and two-photon fluorescence microscopes.[5,15]

3. *Empirical:* If the functional description of the inner product is not available, the basis modes can be orthogonalized using an empirical process in which the form of the metric function is determined from image measurements. A sequence of images is acquired with different bias aberrations applied by the adaptive element. The corresponding metric measurements map out the shape of the metric function in the vicinity of the paraboloidal peak. The new modes are obtained as a linear combination of the basis modes by finding the coordinate system that aligns the primary axes of the paraboloidal maximum with the coordinate axes. This approach has been demonstrated in structured illumination, two-photon and harmonic generation microscopes.[5,15,16] One possible implementation of this empirical method is outlined in the next section.

The analytical approach is applicable to a very limited range of systems. The numerical approach has wider use and could be used with non-analytic basis functions, such as the deformation modes of a deformable mirror. However, this requires an accurate numerical model of the mirror properties and full specification of other system parameters. The empirical approach is more widely applicable, as it could be applied to any sensorless system, as long as the metric has a paraboloidal maximum. This method does not require full specification of the system nor an accurate model of the deformable mirror properties.

## 9. AN EMPIRICAL APPROACH FOR THE DERIVATION OF OPTIMAL MODES

It is possible to obtain optimal modes through experimental measurements, avoiding the need for a mathematical description of the inner product. One method for achieving this is presented in this section. In principle, this involves analysing a set of measurements of the metric $M$ with different applied bias aberrations. From these measurements, one can obtain the shape of the metric function and determine the orientation of the paraboloid, encoded in the coefficients $\alpha_{i,j}$ of Eq. 5. In turn this enables the derivation of the optimal modes.

We choose a set of basis modes $X_i$, the definition of which can be arbitrary at this point – typically one would choose either Zernike modes or a set derived from the properties of the adaptive element, such as mirror deformation modes. We assume that the modes have zero mean value are all normalized to have a root-mean-square phase of 1 rad. We also assume that the basis modes do not contain components of tip, tilt and defocus; as these components correspond to three-dimensional images shifts they should be excluded from AO correction in a three-dimensionally resolved microscope system.

For any pair of basis modes with $i \neq j$, the metric value is measured for a number of test aberrations $\Phi_{(i,j),n}$, which contain certain combinations of the modes $X_i$ and $X_j$. The mode combinations are chosen to have a constant total magnitude $\gamma$ so that the $n$th test aberration is

$$\Phi_{(i,j),n} = \gamma \ \left[\cos\left(\frac{2\pi}{N}n\right) \ X_i + \sin\left(\frac{2\pi}{N}n\right) \ X_j\right] \tag{15}$$

where $N$ is the total number of test aberrations. The constant $\gamma$ should be chosen small enough such that the assumption of small aberration magnitude is valid; a root-mean-square phase value of less than 0.5 rad is usually appropriate. In terms of the shape of the metric function, the $N$ measurements represent the height of the function along a circular path a fixed distance away from the peak. This is illustrated in Fig. 6. The collection of $N$ metric measurements form a polar plot, where the measured metric values are interpreted as radial coordinates and the numbers $\frac{2\pi n}{N}$ as angular coordinates. The resulting elliptical plot is a "section" through the multidimensional paraboloidal peak of $M$ that shows the orientation of the paraboloid to the axes. Several of these plots, acquired for different pairs of modes, provide sufficient information to reconstruct $M$ and obtain the principle axes, which correspond to the optimum modes. One can obtain the coefficients $\alpha_{i,j}$ by fitting a multidimensional ellipsoid $\sum_{i,j} \alpha_{i,j} \ a_i \ a_j = C$ into the data points, where $C$ is a constant. An example of this process was initially presented by Débarre *et al.* as applied to an adaptive structured illumination microscope.[15]

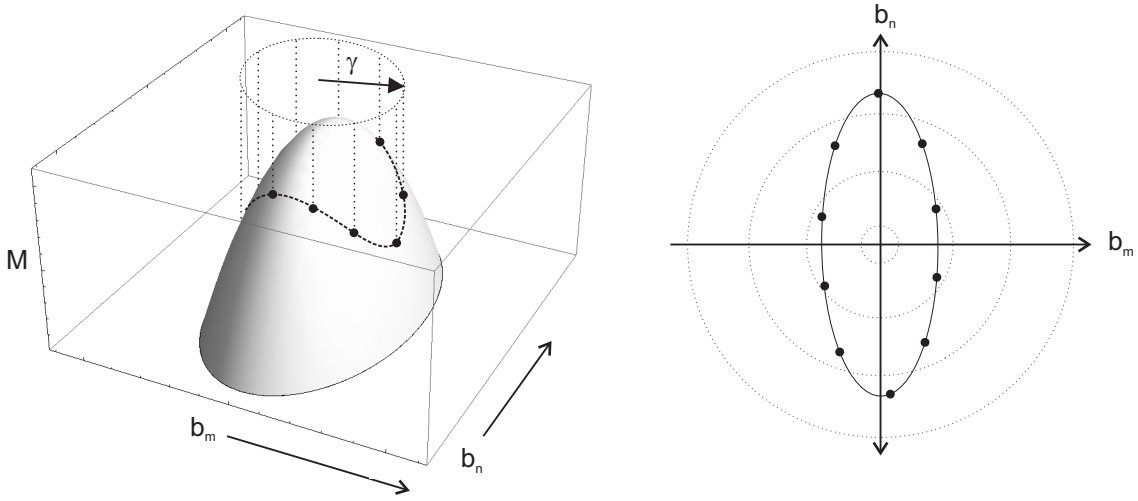


Figure 6. The shape of the multi-dimensional metric ellipsoid can be determined by performing measurements with different test aberrations applied (left image).

The selection of test aberrations is not restricted to the pairs of modes, as explained in the above illustration. It should be possible, for example, to use random combinations of all basis modes to provide random samples of

the metric function. Similarly, one would obtain the coefficients $\alpha_{i,j}$ by fitting a multidimensional ellipsoid to the test points.

## 10. ORTHOGONALIZATION OF MODES

In principle, the set of new aberration modes is derived through orthogonalization of the basis modes. This process uses a particular inner product that depends upon the nature of the imaging system and the choice of optimization metric. In practice, one obtains values of the coefficients $\alpha_{i,j}$ of Eq. 5 either through direct calculation of the inner product or indirectly through empirical measurements, as explained in Section 9. Once the coefficients $\alpha_{i,j}$ have been obtained, the orthogonalization process is facilitated though a matrix formulation. We outline this process as follows. Firstly, we define a matrix $\mathbf{A}$ whose elements are the values of $\alpha_{i,j}$. Equation 5 can then be expressed in the convenient form

$$M \approx M_0 - \mathbf{a}^T \ \mathbf{A} \ \mathbf{a}. \tag{16}$$

where the vector $\mathbf{a}$ consists of the aberration coefficients $a_i$. We then derive an alternative representation by diagonalising $\mathbf{A}$ using a standard eigenvector/eigenvalue decomposition:

$$\mathbf{A} = \mathbf{V} \ \mathbf{B} \ \mathbf{V}^T, \tag{17}$$

where $\mathbf{B}$ is a diagonal matrix, whose on-diagonal entries $\beta_i$ are the eigenvalues of $\mathbf{A}$. The columns of $\mathbf{V}$ are the corresponding eigenvectors. The optimization metric then becomes:

$$M \approx M_0 - \mathbf{a}^T \ \mathbf{V} \ \mathbf{B} \ \mathbf{V}^T \ \mathbf{a} = M_0 - \mathbf{d}^T \ \mathbf{B} \ \mathbf{d} \tag{18}$$

where $\mathbf{d} = \mathbf{V}^T \ \mathbf{a}$. Denoting the elements of the vector $\mathbf{d}$ as $d_i$, we can show that Eq. 18 is now equivalent to the desired form of Eq. 6, where

$$M \approx M_0 - \sum_i \beta_i d_i^2 \tag{19}$$

The values of $d_i$ are the coefficients of the aberration expansion in terms of the optimal modes $Y_i(r,\theta)$, where $\Phi(r,\theta) = \sum_i a_i X_i(r,\theta) = \sum_i d_i Y_i(r,\theta)$. The new modes $Y_i$ can themselves be calculated from the basis modes as

$$Y_i(r,\theta) = \sum_j V_{i,j} X_j(r,\theta) \tag{20}$$

Once the values of $\alpha_{i,j}$ have been found for a particular sensorless AO system, it is therefore a simple mathematical procedure to obtain a new set of orthogonal modes that are optimal for that system.

## 11. CONCLUSION

We have explained the motivation behind sensorless adaptive optics based upon modal wavefront sensing, described the basic principles of the approach and provided an outline of its mathematical basis. We presented in particular a method using sequential quadratic maximization, which has already proven to be effective in a range of adaptive microscopes. Central to this approach is the choice of aberration expansion in terms of modes that are orthogonal, where the definition of orthogonality depends upon the imaging properties of the microscope and the optimization metric. This means that, in general, different sets of optimum modes are required for different adaptive microscopes.

The sensorless adaptive schemes are designed to be specimen independent. Whilst the value of the optimization metric depends upon both aberrations and the specimen structure, the orthogonal form of the metric function does not change if the aberration modes are appropriately chosen. As explained in Section 5, the coefficients of the metric function depend upon factors such as specimen structure, illumination intensity and detection efficiency. This means that the width of the parabolic function can change between different specimens and image settings. However, the metric function retains the necessary form that permits independent optimization of each aberration mode.

It should be emphasized that once the optimum modes have been determined, the aberration measurement and correction process is fast, limited only be the rate at which images can be acquired. Calculations are not usually the speed limiting factor, as neither the evaluation of the quality metric nor the maximization calculation of Eq. 4 are time consuming.

For the purposes of live specimen imaging, it is also important to consider the cumulative exposure during the correction process. When using an image quality metric such as total intensity, the value is averaged across the large number of image pixels. It follows that the image quality required for this measurement could be considerably lower than that required in the final image. The sequence of images used for the aberration correction process can be acquired at higher frame rates and lower illumination intensity than would normally be required for imaging. As an example, it was shown by Débarre *et al.*[5] in an adaptive two-photon microscope that the total cumulative energy dose during correction was only twice the energy dose used in the final image acquisition.

Efficient optimization algorithms are not limited to the sequential quadratic maximization approach explained here. In some systems, it is possible to determine the aberrations using fewer measurements. For example, it has been shown that the system in Section 7 actually requires only $N+1$ measurements to find $N$ modal coefficients.[7] As it is based upon the approximation of Eq. 11, the method is limited in the range of aberration amplitudes that can be corrected. When the aberration amplitude lies near but outside of this range of approximation, the method still provides rapid convergence, but extra iterations may be required before acceptable correction is obtained. Further iterations may also be required if the modes used are not optimum, according to the definition we have used here. This has been shown in confocal and harmonic generation microscopes, where Zernike modes were used in an efficient, but non-optimum sensorless scheme.[4,17] The methods described here could also be combined with more advanced control strategies in order to refine performance in practical adaptive systems.[18]

## Acknowledgements

M. J. Booth was an Engineering and Physical Sciences Research Council (EPSRC) Advanced Research Fellow supported by the grant EP/E055818/1.

## REFERENCES

1. J. W. Hardy, *Adaptive Optics for Astronomical Telescopes*, Oxford University Press, 1998.
2. P. Hariharan, *Optical Interferometry*, Academic Press, 2003.
3. M. J. Booth, "Adaptive optics in microscopy," *Philosophical Transactions Of The Royal Society A-Mathematical Physical And Engineering Sciences* **365**, pp. 2829–2843, Dec. 2007.
4. A. Jesacher, A. Thayil, K. Grieve, D. Dèbarre, T. Watanabe, T. Wilson, S. Srinivas, and M. Booth, "Adaptive harmonic generation microscopy of mammalian embryos.," *Opt Lett* **34**, pp. 3154–3156, Oct 2009.
5. D. Débarre, E. J. Botcherby, T. Watanabe, S. Srinivas, M. J. Booth, and T. Wilson, "Image-based adaptive optics for two-photon microscopy," *Optics Letters* **34**, pp. 2495–2497, Aug. 2009.
6. P. Kner, J. W. Sedat, D. A. Agard, and Z. Kam, "High-resolution wide-field microscopy with adaptive optics for spherical aberration correction and motionless focusing.," *J Microsc* **237**, pp. 136–147, Feb 2010.
7. M. J. Booth, "Wave front sensor-less adaptive optics: a model-based approach using sphere packings," *Optics Express* **14**, pp. 1339–1352, 2006.
8. L. Sherman, J. Y. Ye, O. Albert, and T. B. Norris, "Adaptive correction of depth-induced aberrations in multiphoton scanning microscopy using a deformable mirror," *J. Microsc.* **206**(1), pp. 65–71, 2002.
9. A. J. Wright, D. Burns, B. A. Patterson, S. P. Poland, G. J. Valentine, and J. M. Girkin, "Exploration of the optimisation algorithms used in the implementation of adaptive optics in confocal and multiphoton microscopy," *Microscopy Research and Technique* **67**, pp. 36–44, 2005.
10. F. Zernike, "Beugungstheorie des Schneidenverfahrens und seiner verbesserten Form, der Phasenkontrastmethode," *Physica (Utrecht)* **1**, pp. 689–704, 1934.
11. M. Born and E. Wolf, *Principles of Optics*, Pergamon Press, 6th ed., 1983.
12. W. Press, S. Teukolsky, W. Vetterling, and B. Flannery, *Numerical Recipes in C*, Cambridge University Press, 2nd ed., 1992.

13. M. J. Booth, "Wavefront sensorless adaptive optics for large aberrations," *Opt. Lett.* **32**(1), pp. 5–7, 2007.
14. D. Débarre, M. J. Booth, and T. Wilson, "Image based adaptive optics through optimisation of low spatial frequencies," *Optics Express* **15**, pp. 8176–8190, 2007.
15. D. Débarre, E. J. Botcherby, M. J. Booth, and T. Wilson, "Adaptive optics for structured illumination microscopy.," *Opt Express* **16**, pp. 9290–9305, Jun 2008.
16. N. Olivier, D. Débarre, and E. Beaurepaire, "Dynamic aberration correction for multiharmonic microscopy.," *Opt Lett* **34**, pp. 3145–3147, Oct 2009.
17. M. J. Booth, M. A. A. Neil, R. Juškaitis, and T. Wilson, "Adaptive aberration correction in a confocal microscope," *Proc. Nat. Acad. Sci.* **99**(9), pp. 5788–5792, 2002.
18. H. Song, R. Fraanje, G. Schitter, H. Kroese, G. Vdovin, and M. Verhaegen, "Model-based aberration correction in a closed-loop wavefront-sensor-less adaptive optics system," *Optics Express* **18**, pp. 24070–24084, Nov. 2010.